



# Unbiased Analysis of Temporal Changes in Immune Serum Markers in Acute COVID-19 Infection With Emphasis on Organ Failure, Anti-Viral Treatment, and Demographic Characteristics

OPEN ACCESS

**Edited by:**

Samithamby Jey Jeyaseelan,  
Louisiana State University,  
United States

**Reviewed by:**

Rahul Vijay,  
The University of Iowa, United States  
Dipyaman Ganguly,  
Indian Institute of Chemical Biology  
(CSIR), India

**\*Correspondence:**

Krzysztof Laudanski  
klaudanski@gmail.com

**Specialty section:**

This article was submitted to  
Inflammation,  
a section of the journal  
*Frontiers in Immunology*

**Received:** 07 January 2021

**Accepted:** 10 May 2021

**Published:** 11 June 2021

**Citation:**

Laudanski K, Jihane H, Antalosky B,  
Ghani D, Phan U, Hernandez R,  
Okeke T, Wu J, Rader D and Susztak K  
(2021) Unbiased Analysis of  
Temporal Changes in Immune  
Serum Markers in Acute COVID-19  
Infection With Emphasis on Organ  
Failure, Anti-Viral Treatment, and  
Demographic Characteristics.  
*Front. Immunol.* 12:650465.  
doi: 10.3389/fimmu.2021.650465

Krzysztof Laudanski<sup>1,2,3\*</sup>, Hajj Jihane<sup>4</sup>, Brook Antalosky<sup>5</sup>, Danyal Ghani<sup>5</sup>, Uyen Phan<sup>5</sup>, Ruth Hernandez<sup>5</sup>, Tony Okeke<sup>6</sup>, Junnan Wu<sup>7,8</sup>, Daniel Rader<sup>7,8</sup> and Katalin Susztak<sup>7,8</sup>

<sup>1</sup> Department of Anesthesiology and Critical Care, The University of Pennsylvania, Philadelphia, PA, United States,

<sup>2</sup> Leonard Davis Institute for Healthcare Economics, The University of Pennsylvania, Philadelphia, PA, United States,

<sup>3</sup> Department of Neurology, The University of Pennsylvania, Philadelphia, PA, United States, <sup>4</sup> School of Nursing, Widener University, Philadelphia, PA, United States, <sup>5</sup> College of Arts and Sciences, Drexel University, Philadelphia, PA, United States,

<sup>6</sup> School of Biomedical Engineering, Drexel University, Philadelphia, PA, United States, <sup>7</sup> Department of Genetics, The University of Pennsylvania, Philadelphia, PA, United States, <sup>8</sup> Department of Nephrology, The University of Pennsylvania, Philadelphia, PA, United States

Identification of novel immune biomarkers to gauge the underlying pathology and severity of COVID-19 has been difficult due to the lack of longitudinal studies. Here, we analyzed serum collected upon COVID-19 admission (t1), 48 hours (t2), and seven days later (t3) using Olink proteomics and correlated to clinical, demographics, and therapeutic data. Older age positively correlated with decorin, pleiotrophin, and TNFRS21 but inversely correlated with chemokine (both C-C and C-X-C type) ligands, monocyte attractant proteins (MCP) and TNFRS14. The burden of pre-existing conditions was positively correlated with MCP-4, CAIX, TWEAK, TNFRS12A, and PD-L2 levels. Individuals with COVID-19 demonstrated increased expression of several chemokines, most notably from the C-C and C-X-C family, as well as MCP-1 and MCP-3 early in the course of the disease. Similarly, deceased individuals had elevated MCP-1 and MCP-3 as well as Gal-9 serum levels. LAMP3, GZMB, and LAG3 at admission correlated with mortality. Only CX3CL13 and MCP-4 correlated positively with APACHE score and length of stay, while decorin, MUC-16 and TNFRSF21 with being admitted to the ICU. We also identified several organ-failure-specific immunological markers, including those for respiratory (IL-18, IL-15, Gal-9) or kidney failure (CD28, VEGF). Treatment with hydroxychloroquine, remdesivir, convalescent plasma, and steroids had a very limited effect on the serum variation of biomarkers. Our study identified several potential targets related to COVID-19

heterogeneity (MCP-1, MCP-3, MCP-4, TNFR superfamily members, and programmed death-ligand), suggesting a potential role of these molecules in the pathology of COVID-19.

**Keywords:** COVID-19, remdesivir, convalescent plasma, hydroxychloroquine, steroids, MCP, CCL23, programmed death

## BACKGROUND

Individuals infected with severe acute respiratory syndrome coronavirus 2 (SARS-CoV-2; COVID-19) can be asymptomatic or exhibit mild to morbid symptoms depending on viral load and individual characteristics (1–5). Blood pressure variation, impairments in oxygenation delivery, and metabolomics disruptions are examples of culprits seen in COVID-19 viral septicemia (3, 6, 7). The evolution and characteristics of immune system activation are critical for determining the overall clinical outcomes of SARS-CoV-2 infection and other critical care illnesses, as well as the emergence of failure of specific organs (7–16). For example, it has been observed that lung function deteriorates by the direct cytotoxic effect of the virus and local inflammation governed by monocyte, T cells, and neutrophils during viral sepsis, including SARS-CoV-2 (6, 17–19). In another example, kidney function impairment in COVID-19 is triggered by vascular dysfunction and monocyte activation, which seemed to have distinct immune characteristics as compared to those seen in other organ failures (12, 14, 15, 17). The emergence of the brain's failure is linked to specific endothelial inflammation modulated by leukocytes (17, 20, 21). These dysfunctions may be related to the influx of highly activated monocyte and T-cells into any of the organs and potentiate pathological consequences for COVID-19. Alternatively, immune system markers signify organ failures without being a cause of dysfunction (21).

So far, most of the analysis of COVID-19 inflammation and end-organ failures had focused on global dysfunction, primarily when proteomics serum analysis was employed (22). Other analyses suffered from a small sample size (23). The large-scale proteomics analysis's primary goal is to deliver clues to potential mechanisms leading to disease pathology, especially if combined with longitudinal analysis of marker dynamics (1, 11, 23, 24). However, such studies generate large amounts of data that are often difficult to put in the context of illness. Our study addresses this knowledge gap by focusing on selected monocyte and T cell activation biomarkers as suggested in editorial and reviews and some preliminary studies (4, 6, 12, 13, 25–27). Furthermore, the initial targets are infrequently examined for the causative role. Here, we applied a different approach than multi-omics analysis to be the hypothesize-driven targeted approach to a set of biomarkers.

The treatments in COVID-19 should modulate the direct viral cytotoxicity and immune system response to infection (7, 28, 29). The ideal therapy for viral septicemia should reverse immune dysfunctions, normalize immunological mediators, and reverse organ failures (7, 11, 24). However, it is unclear how any proposed treatments for COVID-19 would alter the immunological

reaction in the yet-to-be-described immunological landscape of the COVID-19 disease. So far, most of the trials failed to deliver a cure (hydroxychloroquine, convalescent plasma) (30–32). Some have significant clinical gains (remdesivir) or were demonstrated to benefit a specific subsequent of patients (steroids) (32–36). Regardless of clinical efficacy, their effects on modulating immunological serum signatures remain mostly unknown. We hypothesize that by analyzing the effect of the COVID-19 treatment on the immune system activation profile, we will discern potential key mechanisms leading to recovery due to the implemented therapy.

In summary, we sought to analyze immunological profile markers related to monocyte and T cells activation during immune system activation using unbiased quantitative targeted proteomics during the evolution of COVID-19. We planned to relate observed changes to demographic variables, pre-existing comorbidities, clinical status, organ dysfunction, COVID-19 outcomes, and treatment. The goal was to identify potential targets linked to the emergence of COVID-19 organ dysfunctions for future research and therapy.

## MATERIALS AND METHODS

### Study Population

Our study protocol was authorized by the Institutional Review Boards (IRBs) of the University of Pennsylvania and was performed according to the ethical guidelines of the 2003 Helsinki Declaration. Written informed consent was obtained from all enrolled patients.

The electronic medical records (EMR) EPIC was used to collect the demographic and medical data on all the enrolled participants. Patients self determined race and ethnicity. The Acute Physiology And Chronic Health Evaluation II (APACHE II) was calculated within one hour ( $APACHE_{1hr}$ ) and at 24 hours after admission ( $APACHE_{24hrs}$ ) (37). The burden of chronic disease was calculated as Charlson Comorbidity Index (CCI) (38). The severity of the illness was determined by Marshalls Organ Dysfunction Score (MODS) and Sequential Organ Failure Assessment (SOFA) (39). The survival was determined at 28 days.

Data regarding therapies with ventilatory support, renal replacement therapy (RRT), and extra-corporeal membrane (ECMO) were retrieved. The status of organ failures was characterized using a framework from the GlueGrant and organ dysfunction scores (39–41). Central Nervous System failure (CNS<sub>f</sub>) was determined as an altered mental status secondary to acute cerebrovascular accident, seizure, or delirium lasting over

72 hours. Respiratory failure ( $R_f$ ) was defined as a condition that requires biphasic non-invasive ventilation, intubation, or ECMO engagement. Cardiovascular failure ( $CVS_f$ ) was determined among patients with shock requiring vasopressors. Liver failure ( $L_f$ ) was identified in patients with severely elevated alanine aminotransferase (ALT), aspartate aminotransferase (AST), total bilirubin, or ammonia levels. Renal failure ( $AKI_f$ ) was determined by serum creatinine from baseline. Hematological failure ( $B_f$ ) was determined when hemoglobin measured less than 9[g%], or increased blood products.

We investigated the engagement of hydroxychloroquine, remdesivir, convalescent plasma, and steroids. Except for the latter, the treatments were highly protocolized per hospital policy according to the FDA recommendations for the given treatment. The presence of steroid treatment was determined as the engagement of any intravenous or oral glucocorticoid steroid compounds to treat COVID-19 pneumonia per healthcare provider notes, according to COVID-19 specific hospital policy.

## Sample Collection and Processing

Blood was drawn at three different time intervals ( $t_{\text{baseline}}$ ; n=36), followed by 48hours ( $t_{48\text{hrs}}$ ; n=28) and seven days ( $t_{7d}$ ; n=17). Blood was collected in heparinized vacutainer tubes (BD, Franklin Lakes, NJ) and put on ice. Downstream processing of biological specimen was done following BSL-2 enhanced standard. Serum was separated by collecting the top layer after spinning the line at 1000xg, 10 minutes, 4°C within 3 hours from collection. Aliquot serum was stored at -80°C. The serum was inactivated by incubation of 100 $\mu$ l of serum with 5% Tween-20 (Bioworld, Baltimore, MD) for 20 minutes at room temperature. The serum was then either shipped for analysis or locally tested with enzyme-linked immunoassays (ELISA) of interest.

The commercial supplier employed O-link technology to assess the serum level of immunological protein. We selected the specific kit targeting biomarkers based on the preliminary data and literature review (**Supplemental Material 1**) (1, 7, 11, 14, 20, 42, 43). Inactivated serum samples (n=64) collected from patients with COVID-19 were analysed using an Olink panel (OLINK Bioscience, Uppsala, Sweden). The kit provides a microtiter plate for measuring 92 protein biomarkers, with data presented as Normalized Protein Expression (NPX) values plotted against protein concentration (in pg/mL) (44). The obtained results are presented as dimensionless values allowing for comparison of the measured protein across different variables (44). Olink technology does not allow for relating different cytokines to each other (44). IL-6 was measured using a multiplex kit (Theromofisher, Waltham, MA) on MagPix machine (Luminex; Austin, TX). CCL23 and MCP-1 were measured by ELISA (Biolegend, San Diego, CA)

## Statistics

Lavene's test and distribution plots were used to test the normality of variables. Parametric variables will be expressed as mean  $\pm$  SD and compared using *t*-Student. Multiple groups were compared using ANOVA with subsequent *t*-Student tests for intra-group comparisons. For non-parametric variables, median ( $M_e$ ) and interquartile ranges (IR) will be shown with

U-Mann-Whitney statistics employed to compare such variables. Correlations were calculated as  $r^2$ -Pearson momentum. The clustering center was calculated using the k-mean using R package using an unbiased approach to identify subgroups of the markers' serum levels. A double-sided *p*-value less than 0.05 will be considered statistically significant for all tests, but we prioritized a more conservative value of 0.01 or less in most of the analyses. Regression analysis was done with stepwise forward methods. The receiver area operator was calculated using discharge home as a binary predictor. Statistical analyses were performed with R, Statistica 11.0 (StatSoft Inc., Tulsa, OK), and SPSS v26 (IBM, Endicott, NY).

## RESULTS

### Characteristics of Studies Population

Subject demographics and clinical characteristics are shown in **Table 1**. The cohort represents subjects previously reported requiring hospitalization due to COVID-19.

### The Effect of Age, Gender, and Race on the Natural History of COVID-19 Immune System Activation

Patients over the age of 60 showed lower levels of chemotaxis molecules (MCP-1, MCP-4, CCL20, CCL19) shortly after admission, while IL-33, CAIX, DCN, PGF, and PTN were higher (**Figure 1A** and **Supplemental Material 2**). After 7 days this pattern slightly changed. In addition, levels of ANGPT2, CXCL13, LAG3, and MCP-3 were lower, while IL-7, ICOS-L, EGF, and CXCL1 were higher as compared to younger subjects (**Figure 1A** and **Supplemental Material 2**). The correlation between serum level and age was highest for CAIX ( $t_{\text{admission}} r^2[36]=0.448$ ;  $p=0.006$ ;  $t_{+48\text{hr}} r^2[28]=0.557$ ;  $p=0.001$ ), DCN ( $t_{\text{admission}} r^2[36]=0.548$ ;  $p=0.001$ ;  $t_{+48\text{hr}} r^2[28]=0.789$ ;  $p<0.000$ ), ADGRG1 ( $t_{\text{admission}} r^2[36]=0.399$ ;  $p=0.016$ ;  $t_{+48\text{hr}} r^2[28]=0.55$ ;  $p=0.002$ ), CD28 ( $t_{\text{admission}} r^2[36]=0.353$ ;  $p=0.035$ ;  $t_{+48\text{hr}} r^2[28]=0.254$ ;  $p=0.019$ ), Gal-1 ( $t_{\text{admission}} r^2[36]=0.427$ ;  $p=0.009$ ;  $t_{+48\text{hr}} r^2[28]=0.311$ ;  $p=0.107$ ), PD-L1 ( $t_{\text{admission}} r^2[36]=0.307$ ;  $p=0.069$ ;  $t_{+48\text{hr}} r^2[28]=0.408$ ;  $p=0.031$ ), CX3CL1 ( $t_{\text{admission}} r^2[36]=0.404$ ;  $p=0.015$ ;  $t_{+48\text{hr}} r^2[28]=0.509$ ;  $p=0.006$ ), PTN ( $t_{\text{admission}} r^2[36]=0.604$ ;  $p=0.000$ ;  $t_{+48\text{hr}} r^2[28]=0.602$ ;  $p=0.001$ ;  $t_{+7d} r^2[28]=0.503$ ;  $p=0.040$ ).

We did not observe a consistent pattern between males and females upon admission; however, after 48 hours, several molecules were higher in males compared to females, such as ANGPT2, CCL20, CD4, CD8, and NOS3 (**Figure 1B** and **Supplemental Material 2**).

Self-identified African-American individuals had lower serum levels of CD8a, MCP-3, CCL23, GAL, MUC-16, NOS3 and PD-L2, and higher ICOSLG levels (**Figure 1C** and **Supplemental Material 2**). 7 days into the disease's progression, ADA, ICOSL, and PD-L2 were significantly elevated in African-American subjects, but CX3CL1, CXCL1, IL-7, and MCP-2 demonstrated somewhat less significant differences (**Figure 1C** and **Supplemental Material 2**).

**TABLE 1 |** Demographic and clinical characteristics of the studied individuals.

|                                       |                         |                    |           |
|---------------------------------------|-------------------------|--------------------|-----------|
| <b>Age</b>                            | Age [X ± SD]            | 63.1 ± 19.28       |           |
|                                       | Below 60 [%]            | 41.7%              |           |
|                                       | Over 60 [%]             | 58.3%              |           |
| <b>Gender</b>                         | Male [%]                | 52.8%              |           |
|                                       | Female [%]              | 47.2%              |           |
|                                       | Not reported [%]        | 0.0%               |           |
| <b>Race</b>                           | Caucasian [%]           | 16.7% (50% Latino) |           |
|                                       | Black [%]               | 69.4%              |           |
|                                       | Other/unknown/Asian [%] | 13.9%              |           |
| <b>Pre-existing conditions</b>        |                         |                    |           |
| Charleston Comorbidity Index [X ± SD] |                         | 3.8 ± 2.99         |           |
| MI [%]                                |                         | 0.0%               |           |
| CHF [%]                               |                         | 16.7%              |           |
| PVD [%]                               |                         | 8.3%               |           |
| CVA/TIA [%]                           |                         | 13.9%              |           |
| Dementia [%]                          |                         | 8.3%               |           |
| COPD [%]                              |                         | 16.7%              |           |
| CTD [%]                               |                         | 2.8%               |           |
| Peptic ulcer disease [%]              |                         | 5.6%               |           |
| Liver disease [%]                     |                         | 2.8%               |           |
| DM [%]                                |                         | 33.3%              |           |
| Hemiplegia [%]                        |                         | 8.3%               |           |
| CKD [%]                               |                         | 27.8%              |           |
| Solid tumor [%]                       |                         | 11.1%              |           |
| Leukemia [%]                          |                         | 0.0%               |           |
| Lymphoma [%]                          |                         | 0.0%               |           |
| AIDS [%]                              |                         | 0.0%               |           |
| Smoking                               | Smoker [%]              | 38.9%              |           |
|                                       | Nonsmoker [%]           | 61.1%              |           |
| Vaper [%]                             |                         | 0.0%               |           |
| Mortality [%]                         |                         | 27.8%              |           |
| Length of Stay [X ± SD]               |                         | 18.2 ± 20.02       |           |
| ICU [%]                               |                         | 58.3%              |           |
| intubated [%]                         |                         | 44.4%              |           |
| ECMO [%]                              |                         | 16.7%              |           |
| APACHE admission +1hr [X ± SD]        |                         | 12.4 ± 9.11        |           |
| APACHE admission +24hrs [X ± SD]      |                         | 12.8 ± 7.04        |           |
| <b>MOF</b>                            | <b>t1</b>               | <b>t2</b>          | <b>t3</b> |
| CNSf [%]                              | 19.4%                   | 14.3%              | 20.8%     |
| CVf [%]                               | 30.6%                   | 22.9%              | 25.0%     |
| Rf [%]                                | 33.3%                   | 40.0%              | 41.7%     |
| AKlf [%]                              | 22.2%                   | 28.6%              | 25.0%     |
| Lf [%]                                | 66.7%                   | 60.0%              | 58.3%     |
| Bf [%]                                | 58.3%                   | 54.3%              | 66.7%     |

MI, myocardial infarction; CHF, congestive heart failure; PVD, peripheral artery disease; CVA, cerebrovascular accident; TIA, transient ischemic stroke; COPD, chronic obstructive pulmonary disease; CTD, connective tissue disease; DM, diabetes mellitus; CKD, chronic kidney disease; AIDS, acquired immunodeficiency syndrome; ICU, intensive care unit; ECMO, extracorporeal membrane oxygenation; APACHE, acute physiology and chronic health evaluation; CNSf, central nervous system failure; CVf, cardiovascular failure; Rf, respiratory failure; AKlf, renal failure; Lf, lung failure; Bf, blood failure.

## The Effect of Pre-Existing Comorbidities on the Serum Profile of the Immune System Activation

The high burden of pre-COVID-19 comorbidities (CCI) correlated with MCP-4, PCN, DCN, CAIX, TWEAK, and TNFRS12A at admission and 48 hours afterward (**Figure 2A** and **Supplemental File 1**). PD-L2 was strongly linked to CCI at all three time points (**Figure 2B** and **Supplemental File 1**).

The presence of chronic kidney disease (CKD) was associated with two distinct marker patterns. The early pattern showed marked changes at admission and 48 hours later, as demonstrated by changes in IL-15, CD27, TNFRS9, PGF, CAIX, MCP-1, and MCP-4 (**Table 2**). In the delayed pattern at seven days after admission for COVID-19, significant differences were appreciated in serum levels of CD83, KRLD1, VEGFA, NCR, TNFSR24, PD-L2, and IL-12.

| <b>A</b>                      |       | <b>B</b>         |                  | <b>C</b>                     |         |                  |                  |                                 |        |                  |                  |
|-------------------------------|-------|------------------|------------------|------------------------------|---------|------------------|------------------|---------------------------------|--------|------------------|------------------|
| <b>Age</b>                    |       | <b>p&lt;0.05</b> | <b>p&lt;0.01</b> | <b>Gender</b>                |         | <b>p&lt;0.05</b> | <b>p&lt;0.01</b> | <b>Race</b>                     |        | <b>p&lt;0.05</b> | <b>p&lt;0.01</b> |
| Lower as compared to <60 y/o  |       |                  |                  | Lower as compared to female  |         |                  |                  | Lower as compared to caucasian  |        |                  |                  |
| Higher as compared to <60 y/o |       |                  |                  | Higher as compared to female |         |                  |                  | Higher as compared to caucasian |        |                  |                  |
|                               |       | t1               | t2               | t3                           |         | t1               | t2               | t3                              |        | t1               | t2               |
| ADGRG1                        |       |                  | 0.001            |                              | ANGPT2  |                  | 0.028            | 0.014                           | ADA    | 0.018            | 0                |
| ANGPT2                        |       |                  |                  |                              | CAIX    | 0.043            |                  |                                 | ARG    |                  | 0.02             |
| CAIX                          | 0.023 | 0.000            |                  |                              | CCL19   |                  | 0.028            |                                 | CCL23  |                  | 0.047            |
| CCL19                         | 0.031 |                  |                  |                              | CCL20   |                  |                  |                                 | CD8A   | 0.008            |                  |
| CCL20                         | 0.018 |                  |                  |                              | CD4     |                  | 0.021            |                                 | CX3CL1 |                  | 0.03             |
| CRTAM                         |       | 0.045            |                  |                              | CDS8A   |                  | 0.002            |                                 | CXCL1  | 0.041            | 0.027            |
| CX3CL1                        |       | 0.039            |                  |                              | CXCL13  |                  |                  |                                 | EGF    | 0.026            |                  |
| CXCL1                         |       |                  | 0.037            |                              | CXCL5   |                  | 0.032            |                                 | Gα1    |                  | 0.021            |
| CXCL11                        | 0.044 |                  |                  |                              | MIC-A/B | 0.034            |                  |                                 | ICOSLG | 0.007            | 0.018            |
| CXCL13                        |       |                  | 0.003            |                              | NOS3    |                  | 0.016            |                                 | IL-7   |                  | 0.022            |
| DCN                           | 0.001 | 0.000            |                  |                              |         |                  |                  |                                 | KLRD1  | 0.043            |                  |
| EGF                           |       |                  | 0.048            |                              |         |                  |                  |                                 | MCP-2  |                  | 0.023            |
| ICOSLG                        |       |                  | 0.007            |                              |         |                  |                  |                                 | MCP-3  |                  | 0.04             |
| IL-15                         |       | 0.040            |                  |                              |         |                  |                  |                                 | MUC-16 | 0.026            | 0.024            |
| IL-33                         | 0.044 |                  |                  |                              |         |                  |                  |                                 | NOS3   | 0.043            | 0.03             |
| IL-7                          |       |                  | 0.005            |                              |         |                  |                  |                                 | PD-L2  | 0.002            | 0.009            |
| LAG3                          |       |                  | 0.017            |                              |         |                  |                  |                                 | TWEAK  | 0.036            |                  |
| MCP-1                         | 0.026 |                  |                  |                              |         |                  |                  |                                 | VEGFA  |                  | 0.023            |
| MCP-3                         |       |                  | 0.029            |                              |         |                  |                  |                                 |        |                  |                  |
| MCP-4                         | 0.002 |                  |                  |                              |         |                  |                  |                                 |        |                  |                  |
| NOS3                          |       |                  | 0.045            |                              |         |                  |                  |                                 |        |                  |                  |
| PGF                           | 0.022 | 0.008            |                  |                              |         |                  |                  |                                 |        |                  |                  |
| PTN                           | 0.003 | 0.011            |                  |                              |         |                  |                  |                                 |        |                  |                  |
| TNFRSF12A                     |       | 0.020            |                  |                              |         |                  |                  |                                 |        |                  |                  |
| TNFRSF21                      |       |                  | 0.047            |                              |         |                  |                  |                                 |        |                  |                  |
| TNFSF14                       | 0.032 |                  |                  |                              |         |                  |                  |                                 |        |                  |                  |

**FIGURE 1 |** Visualization of temporal changes in the variation of the immunological biomarkers when age (cutoff of 60 years) **(A)**, gender **(B)** and race **(C)** were compared across the study subjects. Summary of statistically significant differences demonstrated as higher (red) or lower (blue) than an appropriate comparison group at standard [( $p \leq 0.05$ ); pale shade] and more conservative (darker shade) The mean and SD of the compared group are listed in **Supplemental Material 2**. Denotation of abbreviations and corresponding UniProt number are listed in **Supplemental Material 2**.

## Clinical Outcome and Serum Profile of Immune System Activation

Non-survivors had higher serum levels of MCP-1, CCL23, CXCL10, GZ-MB, LAG3, and LAMP3 as compared to the survival group (**Figures 3A–C** and **Supplemental Material 2**). Gal-9, IL-8, MCP-1, and TNFRS12A were higher in the non-survivor group for 48 hours. It was noteworthy that MCP-1, MCP-3, and Gal-9 remained elevated in non-survivors at 7 days (**Figures 3A, B** and **Supplemental Material 2**). In contrast, ANGPT1 and CCL17 were markedly lower, and IL-6 was higher two and seven days after admission in non-survivors (**Figures 3A, C** and **Supplemental Material 2**). Analysis of the survival identified serum levels of MCP-1, GZMB, LAG3, and LAMP3 at admission were determinants of survival (**Figure 3D**).

However, their ability to predict mortality was relatively low satisfactory in terms of specificity and sensitivity (**Supplemental Figure 1A**). Serum level of EGF at admission demonstrated more satisfactory characteristics to distinguish patients with the ability to be discharged home (**Supplemental Figure 1B**).

Length of stay was best predicted by admission serum level of CCL23, IL-8, GZMB, CD244, GZMH, CCL4, and KIRLD3 (**Supplemental Figure 2**). Admission to the ICU was signified by elevation in several chemokines (CXCL1, CXCL13, MCP-1, MCP-3, CCL23), cytokines (IL-8, IL-15), immunological receptors (PD-L1, PD-L2, LAMP3, LAG3, CD27), TNF $\alpha$  receptor superfamily (TNFRSF12A, TNFRSF4), and stress response markers (HGF, NCR1, MUC-16) (**Figure 4A** and **Supplemental Material 2**). ANGPT1 and CD244 were

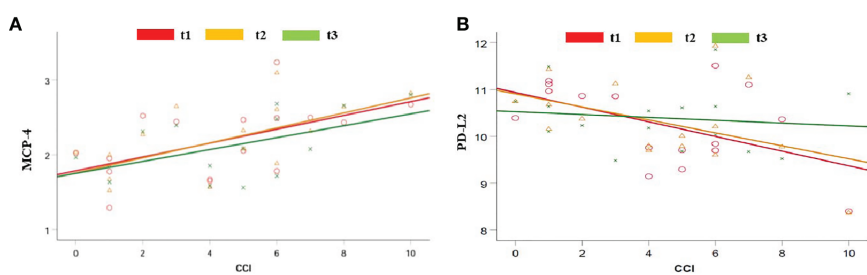


**FIGURE 2 |** Regression analysis between pre-COVID-19 health conditions, calculated as the CCI and serum level of MCP-4 **(A)** and PD-L2 **(B)** when measured at admission (t1; red), 48 hours after admission (t2; yellow) and seven days after admission (t3; green).

**TABLE 2 |** The difference in serum immunological profile between patients with pre-existing CKD during duration of the COVID-19 infection.

| Sample  | No CKD/CKD                      | t1                                | t2                                | t3                               |
|---------|---------------------------------|-----------------------------------|-----------------------------------|----------------------------------|
| IL-15   | No CKD [X ± SD]<br>CKD [X ± SD] | 5.79 ± 0.556<br>5.88 ± 0.901      | **5.80 ± 0.680<br>**6.82 ± 0.326  | *5.83 ± 0.834<br>*6.64 ± 0.519   |
| CD27    | No CKD [X ± SD]<br>CKD [X ± SD] | 8.40 ± 0.497<br>8.72 ± 0.909      | *8.40 ± 0.508<br>*9.08 ± 0.561    | **8.22 ± 0.375<br>**9.09 ± 0.582 |
| CAIX    | No CKD [X ± SD]<br>CKD [X ± SD] | *4.82 ± 0.918<br>*5.65 ± 1.101    | **4.64 ± 0.830<br>**6.14 ± 0.981  | **4.35 ± 0.722<br>**6.18 ± 1.024 |
| MCP-1   | No CKD [X ± SD]<br>CKD [X ± SD] | 11.43 ± 0.791<br>11.42 ± 0.467    | *11.61 ± 0.941<br>*12.66 ± 0.733  | 11.46 ± 1.012<br>12.13 ± 0.800   |
| MCP-4   | No CKD [X ± SD]<br>CKD [X ± SD] | **10.49 ± 0.819<br>**9.55 ± 0.680 | **10.64 ± 0.795<br>**9.62 ± 0.656 | 10.44 ± 0.711<br>10.37 ± 0.579   |
| TNFRSF9 | No CKD [X ± SD]<br>CKD [X ± SD] | *6.24 ± 0.648<br>*6.92 ± 0.993    | **6.05 ± 0.807<br>**7.20 ± 0.987  | 5.88 ± 0.704<br>7.02 ± 1.160     |
| PGF     | No CKD [X ± SD]<br>CKD [X ± SD] | 7.42 ± 0.533<br>8.17 ± 1.225      | **7.33 ± 0.635<br>**8.92 ± 0.863  | **7.17 ± 0.469<br>**8.71 ± 0.800 |
| CD83    | No CKD [X ± SD]<br>CKD [X ± SD] | 3.09 ± 0.456<br>3.47 ± 0.924      | **3.02 ± 0.521<br>**4.05 ± 0.807  | 2.98 ± 0.442<br>3.83 ± 0.908     |
| KRLD1   | No CKD [X ± SD]<br>CKD [X ± SD] | **6.25 ± 0.545<br>**7.28 ± 1.200  | *6.40 ± 0.564<br>*7.09 ± 0.788    | 6.39 ± 0.836<br>7.14 ± 0.882     |
| VEGFA   | No CKD [X ± SD]<br>CKD [X ± SD] | *8.35 ± 0.557<br>*8.86 ± 0.470    | **8.44 ± 0.740<br>**9.20 ± 0.395  | **8.20 ± 0.399<br>**9.03 ± 0.408 |
| NCR1    | No CKD [X ± SD]<br>CKD [X ± SD] | 3.63 ± 0.668<br>4.29 ± 1.211      | *3.61 ± 0.692<br>*4.68 ± 1.112    | 3.45 ± 0.557<br>4.31 ± 0.890     |
| IL-12   | No CKD [X ± SD]<br>CKD [X ± SD] | 5.61 ± 1.163<br>5.18 ± 1.231      | 5.08 ± 1.250<br>5.55 ± 1.023      | 4.86 ± 1.236<br>4.51 ± 0.917     |
| PD-L2   | No CKD [X ± SD]<br>CKD [X ± SD] | 2.10 ± 0.405<br>2.34 ± 0.523      | **2.10 ± 0.436<br>**2.71 ± 0.218  | **1.91 ± 0.271<br>**2.66 ± 0.117 |

\*denote p value between CKN and non-CKD CKD at given time point between 0.05 and 0.01. \*\*denote p value between CKD and non-CKD at given time point less than 0.01.

consistently depressed in the serums of the patients admitted to the ICU. Admission serum level of decorin (DCN), natural cytotoxicity triggering receptor 1 (NCR1), CD28, and TNFRSF21 were determinants of admission to the ICU (**Figure 4B**).

A similar serum immunological pattern was seen in patients needing intubation and ventilatory support. Chemokines (CXCL13, MCP-1, MCP-3, CCL20, CCL23), cytokine (IL-15), immunological receptors (CD4, CD27, CD83, LAMP3, PD-L1, PD-L2, PDCD1), TNF $\alpha$  receptor superfamily members

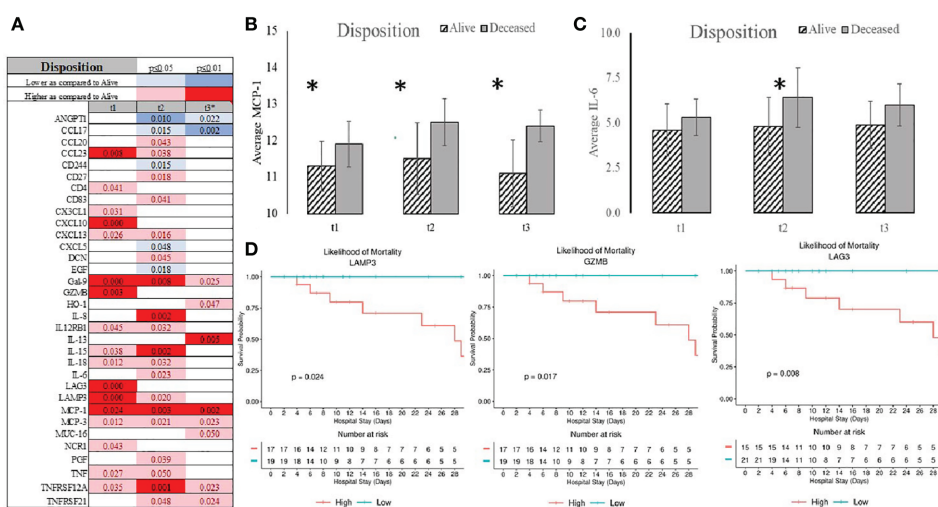


**FIGURE 3 |** Summary of statistically significant differences demonstrated as higher (red) or lower (blue) than an appropriate comparison group at standard [( $p < 0.05$ ); pale shade] and more conservative (darker shade) The mean and SD of the compared group are listed in **Supplemental Material 2**. Denotation of abbreviations and corresponding UniProt number are listed in **Supplemental Material 2**.

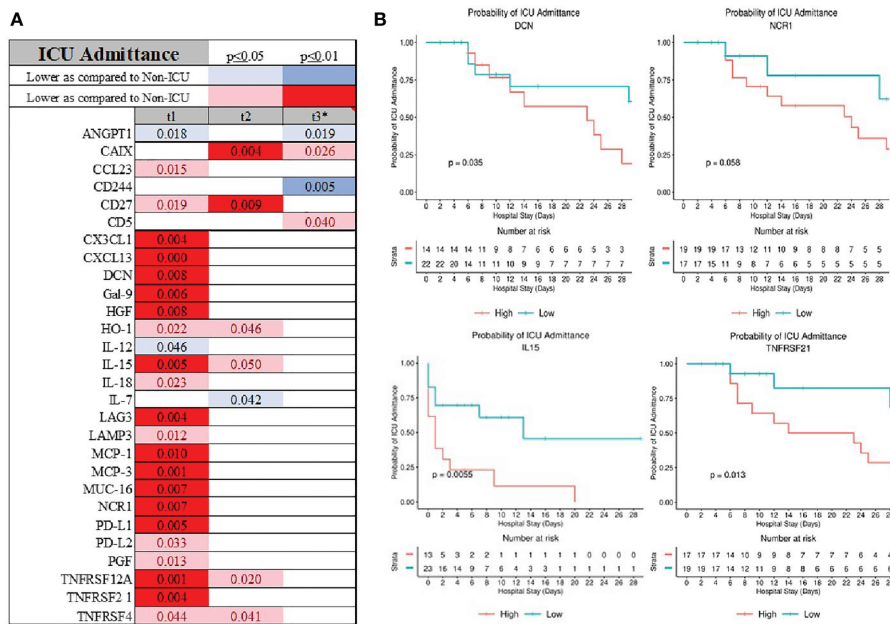


**FIGURE 4** | Also, patients who were admitted to the ICU had distinguish inflammatory profile at the admission (**A**) with DCN, NCR1, IL-15 and TNFRSF21 being good predictor of ICU admission (**B**).

(TNFRSF12A, TNFRSF4), and HGF were elevated in patients needing intubation (**Figure 5A** and **Supplemental Material 2**). Concomitantly, ANGPT1, CCL17, CD244, and EGF were lower, but only ANGPT1 had consistently and statistically significantly

depressed serum levels (**Figure 5A** and **Supplemental Material 2**). TNF $\alpha$ , IL-10, IL-12, IL-18, and IFN $\gamma$  were higher - but only seven days into ICU admission as compared to the non-intubated patients (**Figure 5A** and **Supplemental Material 2**). Finally,

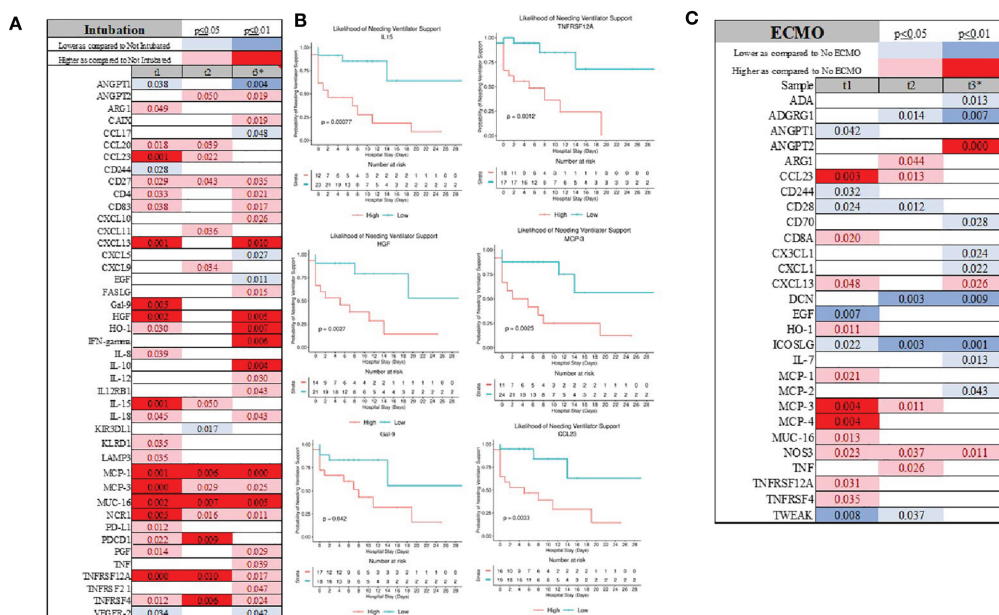


**FIGURE 5** | Intubation was signified for several markers (**A**) which also discriminate patient at the admission for those requiring ventilatory support (**B**). The profile of patient requiring ECMO was significantly different considering large number of inflammatory marker being depressed as compared to patient not requiring ECMO (**C**).

initial serum levels of IL-15, HGF, MCP-3, Gal-9, CCL23, and TNFRSF12A were distinguished patients needing ventilatory support with more favorable outcomes (**Figure 5B**).

Patients who required ECMO showed distinct immunological patterns as signified by lower serum levels of CD28, CD224, and ICOS-L as compared to the non-ECMO group (**Figure 5C** and **Supplemental Material 2**). ANGPT1 was also detectable at a lower level, a similar pattern as that shown in the patients requiring intubation (Supplemental Material 2). As compared to an intubated group, CXCL13, MCP-1, MCP-3, and CCL23 were also elevated. The most striking discovery in the ECMO group was the decrease in several markers at seven days (t3) after admission to the hospital, including ADA, ADGRG1, CD70, CX3CL1, CXCL1, IL-7, and MCP-2, while ANGPT2 was significantly elevated (**Figure 5C** and **Supplemental Material 2**).

Admission APACHE score correlated strongly with serum Gal-9, CX1CL3, TNFRSF12A, TNFRSF21, PGF, CXCL13, Gal-1, DCN, CD27, and CCL23 levels. ANGPT, GZMA, and MCP-4 exhibited strong negative correlations with the illness severity index at admission (**Figure 6A** and **Supplemental Pivot Table 1**). Length of stay, APACHE, SOFA, and MODS was associated with serum level of CXCL13 and CCL23 (**Figures 6A–E** and **Supplemental Pivot Table 1**). MCP-4 correlated positively with LOS but negatively with APACHE (**Figures 6A, D**). Admission serum IL-6 level correlated with overall length of stay ( $r^2[36]=0.36$ ;  $p=0.037$ ), but not with admission APACHE ( $r^2[36]=-0.12$ ;  $p=0.487$ ), MODS ( $r^2[36]=0.145$ ;  $p=0.398$ ), or SOFA ( $r^2[36]=0.102$ ;  $p=0.553$ ) (**Supplemental Pivot Table 1**).

## End Organ Failure and Serum Patterns of Organ Failures

Patients with cardiovascular failure and hypotension requiring intravenous pressors showed lower IL-7 levels later in their COVID-19 trajectory, while CXCL5, IL-12, and ANGPT-1 levels were depressed early during the course of infection

(**Figure 7A; Supplemental Figure 1A** and **Supplemental Material 2**). CD40, CXCL5 and IL-12 were the lone markers exclusively altered at admission if a patient presented with CV only. Patients presented with central nervous system failure showed increased ARG-1, CX3CL1, and DCN, but lower serum expression of EGF at admission (**Figure 7B; Supplemental Figure 1** and **Supplemental Material 2**). The most striking feature of liver failure was the elevation of CCL23, FGF2, and KRLD1 and depression of KIR3DL1 at admission, while Gal-1 and DCN were decreased later during the history of COVID-19 (**Figure 7C** and **Supplemental Material 2**). KIR3DL1 and CXCL9 were unique markers for liver failure (**Supplemental Figure 1B**). Anemia was not related to specific immune system activation patterns in serum (data not shown).

Respiratory failure was signified by depression of EGF, GZMA, LAP, IL-4, and IL-7, and increased expression of MUC-16, ARG-1, and LAMP-3 (**Figure 8A** and **Supplemental Figure 1** and **Supplemental Material 2**). Depression in GRZMA was unique for Rf at admission (**Supplemental Figure 1B**). Finally, admission serum TNFRSF21, IL-18, Gal-9, and CXCL13 were associated with a respiratory decline during hospital stay (**Figure 8B**).

The emergence of AKI was demonstrated by elevated expression of VEGFA, CD28, TNFRSF21, and KRLD1, while MCP-4 was consistently depressed (**Figure 9A; Supplemental Figure 1** and **Supplemental Material 2**). CAIX, IL-33, MCP, and PD-L2 were uniquely abnormal in patients with AKIf at admission (**Supplemental Figure 1B**). Initial serum level of VEGFA and CD28 determined the emergence of AKI during admission (**Figure 9B**).

We identified several proteins whose levels showed highly dynamic changes during COVID-19 infection (**Supplemental Figures 1A, C**). Elevated levels of CXCL13, MMP-7, Gal-1, PDF, and TNFRS family (TNFRSF21, 12A, 4, and 9) during the first 48 hours after admission to the hospital were present across several failures (**Supplemental Figure 3C**).

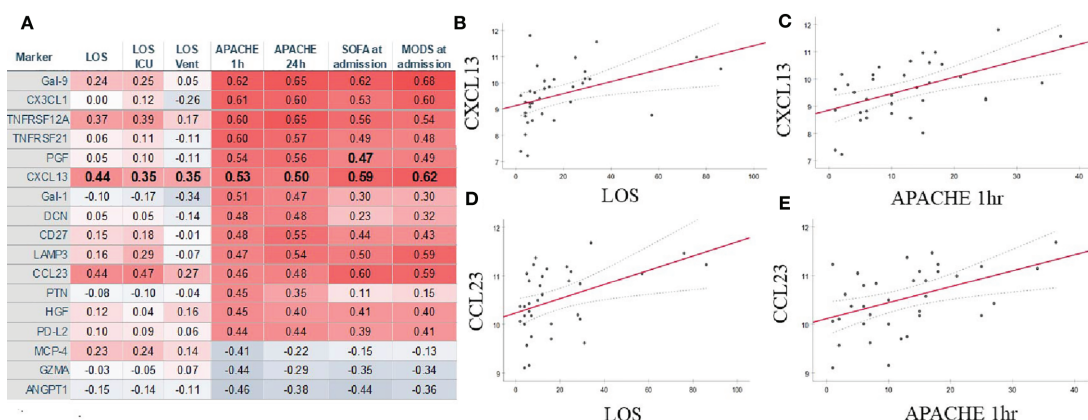


**FIGURE 6** | Several markers correlated strongly with numerous measures of COVID-19 severity (**A**). CXCL-13 (**B, C**) and CCL23 (**D, E**) demonstrated strong correlations with admission APACHE<sub>1hr</sub> (**B, D**) and the length of stay in the hospital (**C, D**). Summary of statistically significant differences demonstrated as higher (red) or lower (blue) correlation. LOS, length of stay; ICU, intensive care unit; Vent, mechanical ventilation; APACHE, acute physiology and chronic health evaluation; SOFA, sequential organ failure assessment; MODS, multiple organ dysfunction syndrome.

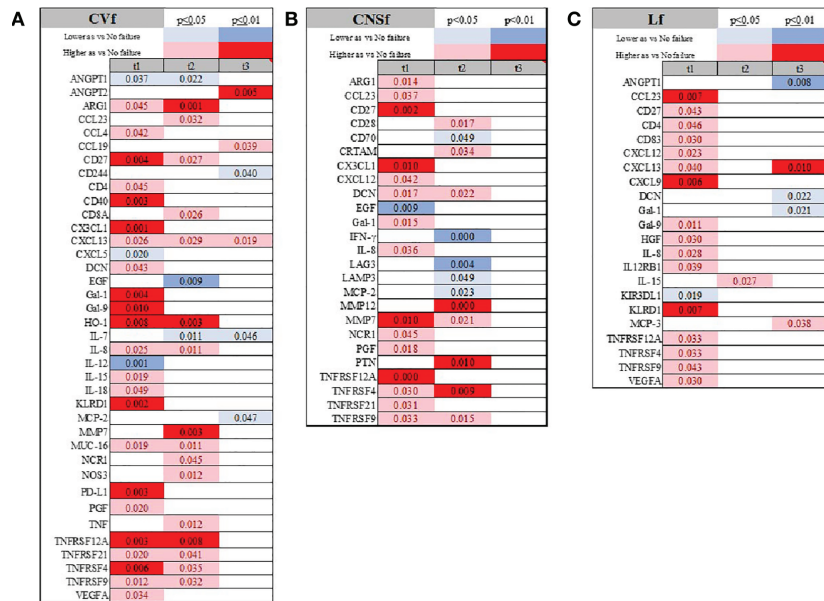


**FIGURE 7** | Time-related temporal markers of the immune system for cardiovascular failure (CVf; A), central nervous system failure (CNSf; B), and liver failure (Lf; C). Summary of statistically significant differences demonstrated as higher (red) or lower (blue) than an appropriate comparison group at standard [( $p \leq 0.05$ ); pale shade] and more conservative (darker shade) The mean and SD of the compared group are listed in **Supplemental Material 2**. Denotation of abbreviations and corresponding UniProt number are listed in **Supplemental Material 2**.

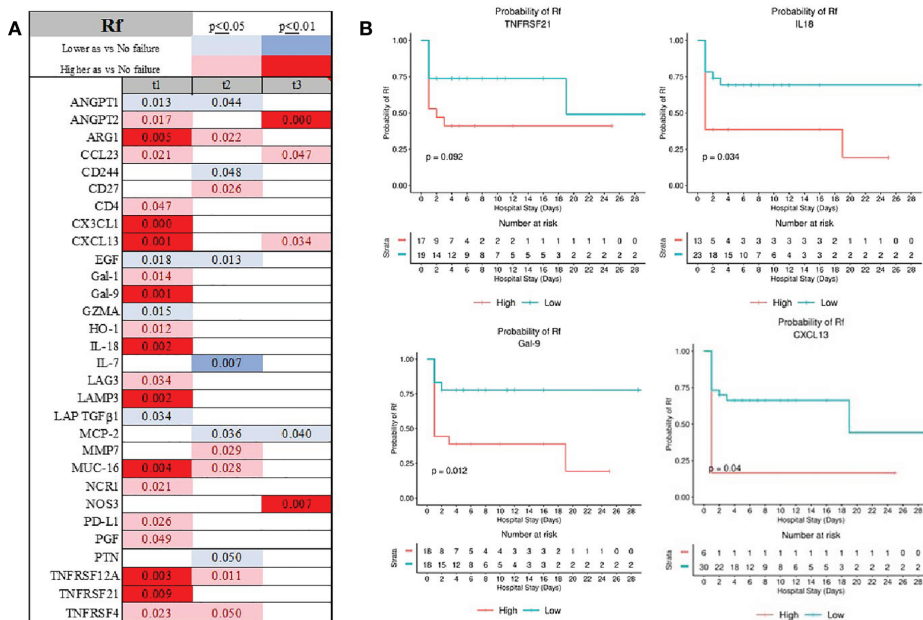


**FIGURE 8** | Time-related temporal markers of the immune system for cardiovascular failure (Rf) (A) demonstrated IL-18, GAL-9, CXCL13 and TNFRSF2 being predictors of patients requiring ventilatory support (B). Summary of statistically significant differences demonstrated as higher (red) or lower (blue) than an appropriate comparison group at standard [( $p \leq 0.05$ ); pale shade] and more conservative (darker shade) The mean and SD of the compared group are listed in **Supplemental Material 2**. Denotation of abbreviations and corresponding UniProt number are listed in **Supplemental Material 2**.

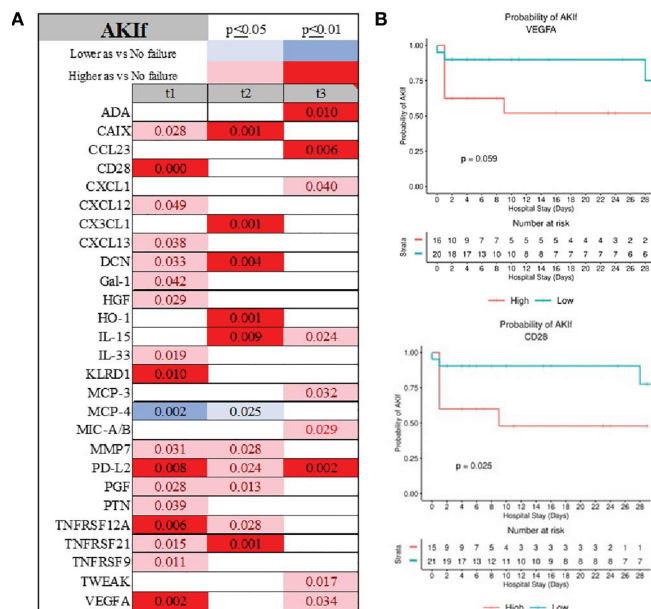


**FIGURE 9 |** Time-related temporal markers of the immune system for cardiovascular failure (AKIif) **(A)** demonstrated VEGFA and CD28 being predictors of patients experiencing acute kidney failure during hospitalization **(B)**. Summary of statistically significant differences demonstrated as higher (red) or lower (blue) than an appropriate comparison group at standard [( $p \leq 0.05$ ); pale shade] and more conservative (darker shade) The mean and SD of the compared group are listed in **Supplemental Material 2**. Denotation of abbreviations and corresponding UniProt number are listed in **Supplemental Material 2**.

## The Effect of the Treatment on the Immunological Profiling

Hydroxychloroquine had an almost negligible effect on most of the markers except for IL-5 (**Figure 10A**). Remdesivir treatment interacted with serum levels of ARG-1, CD28, IL-4, and MCP-1, and MCP3 early at presentation (**Figure 10B** and **Supplemental Figure 4**). Steroids affected Gal-9, IL-12, and MCP-3 early and affected EGF, NOS3, and VEGFR3 levels later in the COVID-19 disease course (**Figure 10C** and **Supplemental Figure 4**). Treatment with convalescent serum interacted with CXCL10, CXCL13, IL-12RB1 and KIR3DL1 (**Figure 10D** and **Supplemental Figure 4**).

## DISCUSSION

Immunological serum profiling revealed that certain biomarkers are virtually uniformly linked to less favorable outcomes (TNFRS12A, TNFRS9, TNFSR21, Gal-1, CD27, MCP family, and CCL23), while others may be related to specific organ injury patterns (CCL4, CD40, CXCL5, and IL-15 for cardiovascular failure; IL-12RB1, KIR3DL1, and CXCL9 for liver failure; CAIX, IL-33, and CXCL9 for kidney failure; GZMA for respiratory failure). EGF was the only predictor of discharge home with somewhat satisfactory operator characteristics. We also noticed remarkable dynamism of the markers throughout the disease. Gender and race differences between different serum markers were present but were of unclear pathophysiological significance. Finally, we

demonstrated the limited effects of the medical therapies on the serum immunological profile.

The predominant activation of several tumor necrosis family members, IL-15, CCL23, NCR1, and CD27 suggests extensive activation of the T cells as well as NK cell (45–47). IL-15, NCR1, and CCL23 are critical for the proliferation of the NK and T cells (25, 45, 48–50). The increased number of the T and NK cells is mainly supported by IL-15 that is critical for preventing activation-induced apoptosis (48, 49). Elevated expression of CD27 significantly augments these processes, as it supports proliferation and inhibits apoptosis (51). Concomitant elevation in TNFRS2 and TNFRS4 further suggests sustained and prolonged T cells' activation (52–55). The net effect is an increase in cell activation and activity, including granzyme release, as demonstrated in our dataset. The results may suggest a surge in the T and NK activity, a frequent observation in COVID patients, and other viral infections (17, 19, 23, 28, 45).

The increase in IL-15 secretion is linked to lung injury in influenza by promoting the influx of CD8<sup>+</sup> T cells (19, 42). Both IL-18 and IL-15 were reported as potential factors contributing to respiratory demise in COVID-19 patients (1, 22, 27, 56). CD27 and increased expression of CXCL13 may support blast response from B cells, as is seen in COVID-19, further propelling vascular inflammation and lung injury (57). This inflammatory process is further fueled by significant activation of the VEGF activation pathways, as seen in our dataset (58). Together with CD27 and TWEAK activation, this is highly suggestive of ongoing vasculitis, a common feature of organ dysfunction in COVID-19 (51, 59, 60).

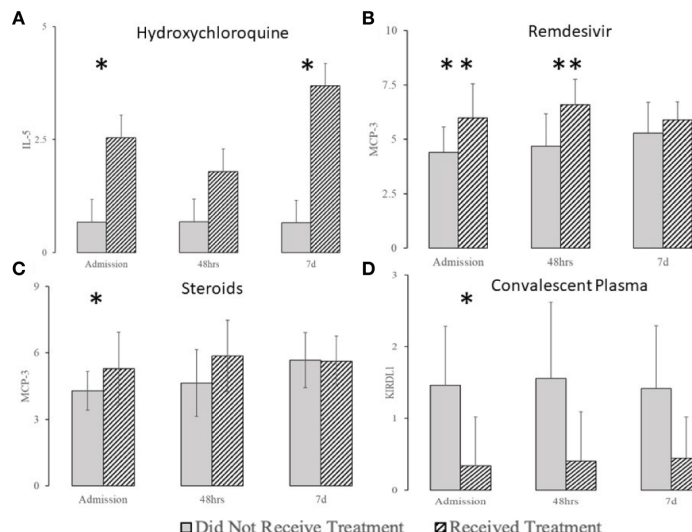


**FIGURE 10 |** The effect of hydroxychloroquine **(A)**, remdesivir **(B)**, steroids **(C)**, and convalescent plasma **(D)** on selected biomarkers (complete list in **Supplemental Figure 2**). \*denotes the difference  $p \leq 0.05$ , \*\*denotes the difference  $p \leq 0.01$ .

The observed pattern of immunological markers resembles the response to viremia in general (19, 47). This profile is highly supportive for recruiting T and NK cells and, to a lesser extend, other leukocytes (MO, neutrophils) into the lung and kidney during inflammation (61, 62). It likely that recruitment may underlie the inflammatory process damaging the end organs in COVID-19 as it is seen in other viral infections where self-sustained autoinflammatory processes emerge (19, 48, 55). The emergence of self-sustained activation of T and NK cells may suggest why COVID-19 extends beyond the initial insult.

We found that process of immune activation is relatively selective. An analysis of cytokine patterns found elevated IL-6 levels, but other cytokines implicated in mediating cytokine storm were not similarly affected. Instead, the immunological activation profile is highly suggestive of the T and NK cell activation instead of widespread activation as often suggested in “cytokine storm” (9, 11, 63). This activation of T cells and NK cells Elevation in Fas and some of the TNFR family implicates high apoptosis activity, suggesting high cell turnover, a typical feature of sepsis (11, 60).

We described several potential organ-specific immune system activation patterns, but their effect on organ failure emergence is unclear (46, 64, 65). The only advent of kidney failure, liver failure, and need for pressors was associated with elevation of specific markers (CCL4, CD40, CXCL5, and IL-15), but our findings’ interpretation needs more broad context (66). Elevation in VEGFA and CD28 in patients with kidney failure suggests its involvement in the emergence of this organ failure (58, 67). Similarly to the lungs, the observed inflammatory profile suggests an environment where T cells and NK are activated. Their migration into lung or kidney tissue may be responsible for the induction of organ dysfunction (68). Our study suggests

potential investigative targets, but the question of their causation in organ failure during COVID-19 is yet to be established.

The effects of treatments were variable and rarely reflected in changes in immunological patterns. Hydroxychloroquine has virtually no impact on immunological serum profile, consistent with its mechanism of action and lack of effectiveness in treating acute COVID-19 (69). Convalescent plasma affected immunological serum profile somewhat, finding coherent evidence of minimal effectiveness (33). Remdesivir suppressed activation of ARG1, soluble CD28, IL-4, IL-7, MCP-1, and MCP-3. These effects are probably secondary to suppressing viral proliferation (70). The effect of steroids was focused on altering IL-12 and MCP-3, yet its linkage to recovery from COVID-19 needs to be established. These results may demonstrate why some of these therapies have limited clinical impact.

The study has several limitations. Perhaps, the most significant one is the exploratory nature of the study. Though we targeted specific immunological markers based on a literature review, our study suggests a potential target without establishing if the marker is the culprit of the COVID-19-related demise or underlying cause (1, 7, 11, 14, 20, 42, 43). Olink technology limits cross-molecule comparisons (44). Hence, our study had to be limited to temporal changes in one marker level without commenting on composition as the difference in concentrations between different immunological modulators (44). Despite this limitation, Olink testing’s robustness was demonstrated by measuring the serum concentration of IL-6 and MCP-1, demonstrating elevation of both cytokines in patients with unfavorable outcomes (22, 27, 40).

The definition of organ failure used a well-established framework, but the data interpretation may be biased secondary to extraction from electronic medical records (40).

Our definitions of organ failure are much more encompassing as compared to more restrictive studies (11, 63). Our study involved a heterogeneous population of patients. This allowed testing several hypotheses across several COVID-19 presentations in the context of comorbidities and demographical variables, yet hampered analysis of these variables on immunological profile, race, and clinical outcomes (28, 34, 41, 71). Race and sex were determined by patients, which is a subject of controversy.

Our study demonstrated significant effects of age and pre-existing renal failure on the immunological profile (28, 34, 41, 71). A more extensive study would be instrumental in accounting for these variables to analyze immunological serum profiles in COVID-19 patients. Some of these variables, like age, have an independent influence on the progression of pneumonia in general, while others (like a renal disease) affect immunological responses (14, 15, 71). Serum measurements may not reflect the molecules' functional activity since we detected shed, released, or secreted molecules (44). These processes can be part of the immune response, transcytosis of a receptor, or molecule release secondary to cytolysis, necrosis, or apoptosis (48). The study is observational, and the result should be considered as hypothesis-generating. Despite that using longitudinal analysis demonstrated high longitudinal variability of the immune markers, the causative effect of any of these changes cannot be determined. A similar problem was seen in prior studies trying to pinpoint markers causative impact in other viral diseases (7, 28, 43). However, several chemokines were reported elevated in COVID-19 and other inflammatory conditions, suggesting, at minimum, potential investigational targets (9, 40, 43, 63). We also took a very conservative approach to analyze our data, frequently calling on statistical significance when the false-positive probability was less than 0.01 instead of the traditional 0.05 value as a cutoff for rejecting the null hypothesis. Finally, we applied multiple statistical methods to more in-depth described the immunological situation of patients.

Our study strongly suggests vibrant T & NK cell response during COVID-19 in our population (7–9, 11). Abnormalities in IL-15, NCR1, CD27, and an increase in T & NK cell activation traits, similar to those observed during swine flu and influenza, were prominent and may be considered a target of further investigation using a more controlled methodology (28). IL-15 was previously suggested to be a potential target in the treatment of COVID-19 viremia (29). When examining the MCP family's role, several chemokines seemed also to be prominent in patients' immunological signatures suggesting activation and trafficking of the MO. To determine causative effects of these molecules in the emergence of the COVID-19 morbidities will require *in vivo* experiments but our study identified several promising targets.

## REFERENCES

1. Ware LB. Physiological and Biological Heterogeneity in COVID-19-associated Acute Respiratory Distress Syndrome. *Lancet Respir Med* (2020) 20:30369–6. doi: 10.1016/S2213-2600(20)30369-6
2. Ren C, Yao RQ, Ren D, Li JX, Li Y, Liu XY, et al. The Clinical Features and Prognostic Assessment of SARS-CoV-2 Infection-Induced Sepsis Among COVID-19 Patients in Shenzhen, China. *Front Med (Lausanne)* (2020) 7:570853. doi: 10.3389/fmed.2020.570853

## DATA AVAILABILITY STATEMENT

The datasets presented in this study can be found in online repositories. The names of the repository/repositories and accession number(s) can be found in the article/**Supplementary Material**.

## ETHICS STATEMENT

The studies involving human participants were reviewed and approved by Institutional Review Board at the University of Pennsylvania. The patients/participants provided their written informed consent to participate in this study.

## AUTHOR CONTRIBUTIONS

KL: study concept, patient recruitment, sample processing, immunological measurements, data analysis, manuscript writing, manuscript review, submission. BA: data analysis, manuscript writing.

DG: data analysis, manuscript writing. RH: data analysis, manuscript writing. HJ: patient consent, sample acquisition clinical data collection. UP: clinical data collections, data analysis, manuscript preparation. TO: data analysis, manuscript preparation. DR: data analysis, manuscript preparation. KS: immunological profile measurements, data analysis, manuscript preparation. All authors contributed to the article and approved the submitted version.

## FUNDING

K23 GM120630, R01 DK105821, R01 DK087635, R01 DK076077.

## ACKNOWLEDGMENTS

We would like to appreciate Joellen Waever and the staff of BioBank at the University of Pennsylvania for creating a structure to support this research.

## SUPPLEMENTARY MATERIAL

The Supplementary Material for this article can be found online at: <https://www.frontiersin.org/articles/10.3389/fimmu.2021.650465/full#supplementary-material>

**Supplementary Table 1** | Pivot table of correlations between biomarkers and clinical indicators.

3. Mathew D, Giles JR, Baxter AE, Greenplate AR, Wu JE, Alanio C, et al. Deep Immune Profiling of COVID-19 Patients Reveals Patient Heterogeneity and Distinct Immunotypes With Implications for Therapeutic Interventions. *bioRxiv* (2020). doi: 10.1101/2020.05.20.106401
4. Pagliaro P. Is Macrophages Heterogeneity Important in Determining COVID-19 Lethality? *Med Hypotheses* (2020) 143:110073. doi: 10.1016/j.mehy.2020.110073
5. The Lancet R. High-Stakes Heterogeneity in COVID-19. *Lancet Rheumatol* (2020) 2(10):e577. doi: 10.1016/S2665-9913(20)30310-6

6. Hue S, Beldi-Ferchiou A, Bendib I, Surenaud M, Fourati S, Frapard T, et al. Uncontrolled Innate and Impaired Adaptive Immune Responses in Patients With COVID-19 Acute Respiratory Distress Syndrome. *Am J Respir Crit Care Med* (2020) 202(11):1509–19. doi: 10.1164/rccm.202005-1885OC
7. Lin GL, McGinley JP, Drysdale SB, Pollard AJ. Epidemiology and Immune Pathogenesis of Viral Sepsis. *Front Immunol* (2018) 9:2147. doi: 10.3389/fimmu.2018.02147
8. Davila S, Halstead ES, Hall MW, Doctor A, Telford R, Holubkov R, et al. Viral DNAemia and Immune Suppression in Pediatric Sepsis. *Pediatr Crit Care Med* (2018) 19(1):e14–22. doi: 10.1097/PCC.0000000000001376
9. Remy KE, Mazer M, Striker DA, Ellebedy AH, Walton AH, Unsinger J, et al. Severe Immunosuppression and Not A Cytokine Storm Characterizes COVID-19 Infections. *JCI Insight* (2020) 5(17):1–15. doi: 10.1172/jci.insight.140329
10. Mudd PA, Crawford JC, Turner JS, Souquette A, Reynolds D, Bender D, et al. Targeted Immunosuppression Distinguishes COVID-19 From Influenza in Moderate and Severe Disease. *medRxiv preprint server Health Sci* (2020). doi: 10.1101/2020.05.28.20115667
11. Hotchkiss RS, Moldawer LL, Opal SM, Reinhart K, Turnbull IR, Vincent JL. Sepsis and Septic Shock. *Nat Rev Dis Primers* (2016) 2:16045. doi: 10.1038/nrdp.2016.45
12. Freaney PM, Shah SJ, Khan SS. Covid-19 and Heart Failure With Preserved Ejection Fraction. *JAMA* (2020) 324(15):1499–500. doi: 10.1001/jama.2020.17445
13. Tomasoni D, Italia L, Adamo M, Inciardi RM, Lombardi CM, Solomon SD, et al. Covid-19 and Heart Failure: From Infection to Inflammation and Angiotensin II Stimulation. Searching for Evidence From A New Disease. *Eur J Heart Fail* (2020) 22(6):957–66. doi: 10.1002/ejhf.1871
14. Wu H, Larsen CP, Hernandez-Arroyo CF, Mohamed MMB, Caza T, Sharshir M, et al. AKI and Collapsing Glomerulopathy Associated With COVID-19 and APOL1 High-Risk Genotype. *J Am Soc Nephrol* (2020) 31(8):1688–95. doi: 10.1681/ASN.2020050558
15. Fisher M, Neugarten J, Bellin E, Yunes M, Stahl L, Johns TS, et al. AKI in Hospitalized Patients With and Without COVID-19: A Comparison Study. *J Am Soc Nephrol* (2020) 31(9):2145–57. doi: 10.1681/ASN.2020040509
16. Sonzogni A, Previtali G, Seghezzi M, Grazia Alessio M, Gianatti A, Licini L, et al. Liver Histopathology in Severe COVID 19 Respiratory Failure is Suggestive of Vascular Alterations. *Liver Int Off J Int Assoc Study Liver* (2020) 40(9):2110–6. doi: 10.1111/liv.14601
17. Zhang J, Tecson KM, McCullough PA. Endothelial Dysfunction Contributes to COVID-19-Associated Vascular Inflammation and Coagulopathy. *Rev Cardiovasc Med* (2020) 21(3):315–9. doi: 10.31083/j.rcm.2020.03.126
18. Goette A, Patschke M, Henschke F, Hammwohner M. Covid-19-Induced Cytokine Release Syndrome Associated With Pulmonary Vein Thromboses, Atrial Cardiomyopathy, and Arterial Intima Inflammation. *TH Open* (2020) 4 (3):e271–e9. doi: 10.1055/s-0040-1716717
19. Verbist KC, Rose DL, Cole CJ, Field MB, Klonowski KD. IL-15 Participates in the Respiratory Innate Immune Response to Influenza Virus Infection. *PloS One* (2012) 7(5):e37539–e. doi: 10.1371/journal.pone.0037539
20. Becker RC. Covid-19-associated Vasculitis and Vasculopathy. *J Thromb thrombolysis* (2020) 50(3):499–511. doi: 10.1007/s11239-020-02230-4
21. DeKosky ST, Kochanek PM, Valadka AB, Clark RSB, Chou SH, Au AK, et al. Blood Biomarkers for Detection of Brain Injury in COVID-19 Patients. *J Neurotrauma* (2021) 38(1):1–43. doi: 10.1089/neu.2020.7332
22. Consiglio CR, Cotugno N, Sardh F, Pou C, Amodio D, Rodriguez L, et al. The Immunology of Multisystem Inflammatory Syndrome in Children With COVID-19. *Cell* (2020) 183(4):968–81.e7. doi: 10.1016/j.cell.2020.09.016
23. Ong EZ, Chan YFZ, Leong WY, Lee NMY, Kalimuddin S, Haja Mohideen SM, et al. A Dynamic Immune Response Shapes COVID-19 Progression. *Cell Host Microbe* (2020) 27(6):879–82.e2. doi: 10.1016/j.chom.2020.03.021
24. Russano M, Citarella F, Napolitano A, Dell'Aquila E, Cortellini A, Pantano F, et al. COVID-19 Pneumonia and Immune-Related Pneumonitis: Critical Issues on Differential Diagnosis, Potential Interactions, and Management. *Expert Opin Biol Ther* (2020) 20(9):959–64. doi: 10.1080/14712598.2020.1789097
25. Younes S-A, Freeman ML, Mudd JC, Shive CL, Reynaldi A, Panigrahi S, et al. IL-15 Promotes Activation and Expansion of CD8+ T Cells in HIV-1 Infection. *J Clin Invest* (2016) 126(7):2745–56. doi: 10.1172/JCI85996
26. Schulte-Schrepping J, Reusch N, Paclik D, Baßler K, Schlickeiser S, Zhang B, et al. Severe COVID-19 is Marked by a Dysregulated Myeloid Cell Compartment. *Cell* (2020) 182(6):1419–40.e23. doi: 10.1016/j.cell.2020.08.001
27. Chevrier S, Zurbuchen Y, Cervia C, Adamo S, Raeber ME, de Souza N, et al. A Distinct Innate Immune Signature Marks Progression From Mild to Severe COVID-19. *Cell Rep Med* (2021) 2(1):100166. doi: 10.1016/j.xcrm.2020.100166
28. Hagau N, Slavcovici A, Gonganau DN, Oltean S, Dirzu DS, Brezoszki ES, et al. Clinical Aspects and Cytokine Response in Severe H1N1 Influenza A Virus Infection. *Crit Care* (2010) 14(6):R203. doi: 10.1186/cc9324
29. Kandikattu HK, Venkateshaiah SU, Kumar S, Mishra A. IL-15 Immunotherapy is A Viable Strategy for COVID-19. *Cytokine Growth Factor Rev* (2020) 54:24–31. doi: 10.1016/j.cytogr.2020.06.008
30. Lewis K, Chaudhuri D, Alshamsi F, Carayannopoulos L, Dearnest K, Chagla Z, et al. The Efficacy and Safety of Hydroxychloroquine for COVID-19 Prophylaxis: A Systematic Review and Meta-Analysis of Randomized Trials. *PLoS One* (2021) 16(1):e0244778. doi: 10.1371/journal.pone.0244778
31. Kim MS, An MH, Kim WJ, Hwang TH. Comparative Efficacy and Safety of Pharmacological Interventions for the Treatment of COVID-19: A Systematic Review and Network Meta-Analysis. *PLoS Med* (2020) 17(12):e1003501. doi: 10.1371/journal.pmed.1003501
32. Cavalcanti AB, Zampieri FG, Rosa RG, Azevedo LCP, Veiga VC, Avezum A, et al. Hydroxychloroquine With or Without Azithromycin in Mild-to-Moderate Covid-19. *New Engl J Med* (2020) 383(21):2041–52. doi: 10.1056/NEJMx200201
33. Simonovich VA, Burgos Pratz LD, Scibona P, Beruto MV, Vallone MG, Vázquez C, et al. A Randomized Trial of Convalescent Plasma in Covid-19 Severe Pneumonia. *New Engl J Med* (2020) 384(7):619–29. doi: 10.1056/NEJMoa2031304
34. Lamontagne F, Agoritsas T, Macdonald H, Leo YS, Diaz J, Agarwal A, et al. A Living WHO Guideline on Drugs for Covid-19. *Bmj* (2020) 370:m3379. doi: 10.1136/bmj.m3379
35. Tomazini BM, Maia IS, Cavalcanti AB, Berwanger O, Rosa RG, Veiga VC, et al. Effect of Dexamethasone on Days Alive and Ventilator-Free in Patients With Moderate or Severe Acute Respiratory Distress Syndrome and COVID-19: The CoDEX Randomized Clinical Trial. *Jama* (2020) 324(13):1307–16. doi: 10.1001/jama.2020.17021
36. Rezagholizadeh A, Khiali S, Sarbakhsh P, Entezari-Maleki T. Remdesivir for Treatment of COVID-19; An Updated Systematic Review and Meta-Analysis. *Eur J Pharmacol* (2021) 897:17392–66. doi: 10.1016/j.ejphar.2021.173926
37. Barie PS, Hydo LJ, Fischer E. Comparison of APACHE II and III Scoring Systems for Mortality Prediction in Critical Surgical Illness. *Arch Surg* (1995) 130(1):77–82. doi: 10.1001/archsurg.1995.01430010079016
38. Buntinx F, Niclaes L, Suetens C, Jans B, Mertens R, Van den Akker M. Evaluation of Charlson's Comorbidity Index in Elderly Living in Nursing Homes. *J Clin Epidemiol* (2002) 55(11):1144–7. doi: 10.1016/S0895-4356(02)00485-7
39. Peres Bota D, Melot C, Lopes Ferreira F, Nguyen Ba V, Vincent JL. The Multiple Organ Dysfunction Score (MODS) Versus the Sequential Organ Failure Assessment (SOFA) Score in Outcome Prediction. *Intensive Care Med* (2002) 28(11):1619–24. doi: 10.1007/s00134-002-1491-3
40. Evans HL, Cuschieri J, Moore EE, Shapiro MB, Nathens AB, Johnson JL, et al. Inflammation and the Host Response to Injury, A Large-Scale Collaborative Project: Patient-Oriented Research Core Standard Operating Procedures for Clinical Care IX. *Definitions complications Clin Care critically injured patients J Trauma* (2009) 67(2):384–8. doi: 10.1097/TA.0b013e3181ad66a7
41. Smiechowicz J. Prognostic Scoring Systems for Mortality in Intensive Care Units – the APACHE Model. *Anaesthesiol Intensive Ther* (2015) 47(1):87–8. doi: 10.5603/AIT.2015.0009
42. Nakamura R, Maeda N, Shibata K, Yamada H, Kase T, Yoshikai Y. Interleukin-15 is Critical in the Pathogenesis of Influenza A Virus-Induced Acute Lung Injury. *J Virol* (2010) 84(11):5574–82. doi: 10.1128/JVI.02030-09
43. Gruber CN, Patel RS, Trachtman R, Lepow L, Amanat F, Krammer F, et al. Mapping Systemic Inflammation and Antibody Responses in Multisystem Inflammatory Syndrome in Children (Mis-C). *Cell* (2020) 183(4):982–95.e14. doi: 10.1016/j.cell.2020.09.034
44. Assarsson E, Lundberg M, Holmquist G, Björksten J, Bucht Thorsen S, Ekman D, et al. Homogenous 96-Plex PEA Immunoassay Exhibiting High

- Sensitivity, Specificity, and Excellent Scalability. *PLoS One* (2014) 9(4):e95192. doi: 10.1371/journal.pone.0095192
45. Elhaik-Goldman S, Kafka D, Yossef R, Hadad U, Elkabets M, Vallon-Eberhard A, et al. The Natural Cytotoxicity Receptor 1 Contribution to Early Clearance of Streptococcus Pneumoniae and to Natural Killer-Macrophage Cross Talk. *PLoS One* (2011) 6(8):e23472. doi: 10.1371/journal.pone.0023472
46. Simats A, García-Berrocoso T, Penalba A, Giralt D, Llovera G, Jiang Y, et al. CCL23: A New CC Chemokine Involved in Human Brain Damage. *J Internal Med* (2018) 283(5):461–75. doi: 10.1111/joim.12738
47. Hayakawa Y, Smyth MJ. CD27 Dissects Mature NK Cells Into Two Subsets With Distinct Responsiveness and Migratory Capacity. *J Immunol* (2006) 176(3):1517–24. doi: 10.4049/jimmunol.176.3.1517
48. Tamzalit F, Barbieux I, Plet A, Heim J, Nedellec S, Morisseau S, et al. IL-15 $\alpha$  Complex Shedding Following Trans-Presentation Is Essential for the Survival of IL-15 Responding NK and T Cells. *Proc Natl Acad Sci United States America* (2014) 111(23):8565–70. doi: 10.1073/pnas.1405514111
49. Liu K, Catalfamo M, Li Y, Henkart PA, Weng NP. IL-15 Mimics T Cell Receptor Crosslinking in the Induction of Cellular Proliferation, Gene Expression, and Cytotoxicity in CD8+ Memory T Cells. *Proc Natl Acad Sci United States America* (2002) 99(9):6192–7. doi: 10.1073/pnas.092675799
50. Milo I, Blecher-Gonen R, Barnett-Itzhaki Z, Bar-Ziv R, Tal O, Gurevich I, et al. The Bone Marrow Is Patrolled by NK Cells That Are Primed and Expand in Response to Systemic Viral Activation. *Eur J Immunol* (2018) 48(7):1137–52. doi: 10.1002/eji.201747378
51. Akiba H, Nakano H, Nishinaka S, Shindo M, Kobata T, Atsuta M, et al. CD27, A Member of the Tumor Necrosis Factor Receptor Superfamily, Activates NF-kappaB and Stress-Activated Protein Kinase/C-Jun N-terminal Kinase via TRAF2, TRAF5, and NF-kappaB-inducing Kinase. *J Biol Chem* (1998) 273(21):13353–8. doi: 10.1074/jbc.273.21.13353
52. Song J, Salek-Ardakani S, Rogers PR, Cheng M, Van Parijs L, Croft M. The Costimulation-Regulated Duration of PKB Activation Controls T Cell Longevity. *Nat Immunol* (2004) 5(2):150–8. doi: 10.1038/ni1030
53. Rogers PR, Song J, Gramaglia I, Killeen N, Croft M. OX40 Promotes Bcl-xL and Bcl-2 Expression and Is Essential for Long-Term Survival of CD4 T Cells. *Immunity* (2001) 15(3):445–55. doi: 10.1016/S1074-7613(01)00191-1
54. Kawamata S, Hori T, Imura A, Takaori-Kondo A, Uchiyama T. Activation of OX40 Signal Transduction Pathways Leads to Tumor Necrosis Factor Receptor-Associated Factor (TRAF) 2- and TRAF5-Mediated Nf- $\kappa$ b Activation. *J Biol Chem* (1998) 273(10):5808–14. doi: 10.1074/jbc.273.10.5808
55. Tam EM, Fulton RB, Sampson JF, Muda M, Camblin A, Richards J, et al. Antibody-Mediated Targeting of TNFR2 Activates CD8(+) T Cells in Mice and Promotes Antitumor Immunity. *Sci Transl Med* (2019) 11(512):1–15. doi: 10.1126/scitranslmed.aax0720
56. Huang W, Li M, Luo G, Wu X, Su B, Zhao L, et al. The Inflammatory Factors Associated With Disease Severity to Predict COVID-19 Progression. *J Immunol* (2021) 206(7):1597–608. doi: 10.4049/jimmunol.2001327
57. Jacquot S, Kobata T, Iwata S, Schlossman SF, Morimoto C. CD27/CD70 Interaction Contributes to the Activation and the Function of Human Autoreactive CD27+ Regulatory T Cells. *Cell Immunol* (1997) 179(1):48–54. doi: 10.1006/cimm.1997.1150
58. Hanna RM, Tran N-T, Patel SS, Hou J, Jhaveri KD, Parikh R, et al. Thrombotic Microangiopathy and Acute Kidney Injury Induced After Intravitreal Injection of Vascular Endothelial Growth Factor Inhibitors Vegf Blockade-Related Tma After Intravitreal Use. *Front Med* (2020) 7(580):1–10. doi: 10.3389/fmed.2020.579603
59. Chen T, Guo ZP, Li L, Li MM, Wang TT, Jia RZ, et al. TWEAK Enhances E-selectin and ICAM-1 Expression, and May Contribute to the Development of Cutaneous Vasculitis. *PLoS One* (2013) 8(2):e56830. doi: 10.1371/journal.pone.0056830
60. Li M, Chen T, Guo Z, Li J, Cao N. Tumor Necrosis Factor-Like Weak Inducer of Apoptosis and Its Receptor Fibroblast Growth Factor-Inducible 14 Are Expressed in Urticular Vasculitis. *J Dermatol* (2013) 40(11):891–5. doi: 10.1111/j.1346-8138.12251
61. Patel VP, Kreider BL, Li Y, Li H, Leung K, Salcedo T, et al. Molecular and Functional Characterization of Two Novel Human C-C Chemokines as Inhibitors of Two Distinct Classes of Myeloid Progenitors. *J Exp Med* (1997) 185(7):1163–72. doi: 10.1084/jem.185.7.1163
62. Hastie AT, Steele C, Dunaway CW, Moore WC, Rector BM, Ampleford E, et al. Complex Association Patterns for Inflammatory Mediators in Induced Sputum From Subjects With Asthma. *Clin Exp Allergy J Br Soc Allergy Clin Immunol* (2018) 48(7):787–97. doi: 10.1111/cea.13129
63. De AK, Miller-Graziano CL, Calvano SE, Laudanski K, Lowry SF, Moldawer LL, et al. Selective Activation of Peripheral Blood T Cell Subsets by Endotoxin Infusion in Healthy Human Subjects Corresponds to Differential Chemokine Activation. *J Immunol* (2005) 175(9):6155–62. doi: 10.4049/jimmunol.175.9.6155
64. Zhang T, Yu J, Wang G, Zhang R. Amyloid Precursor Protein Binds With TNFRSF21 to Induce Neural Inflammation in Alzheimer's Disease. *Eur J Pharm Sci* (2020) (157):15598–05602. doi: 10.1016/j.ejps.2020.105598
65. Raman D, Milatovic S-Z, Milatovic D, Splittergerber R, Fan G-H, Richmond A. Chemokines, Macrophage Inflammatory Protein-2 and Stromal Cell-Derived Factor-1 $\alpha$ , Suppress Amyloid  $\beta$ -Induced Neurotoxicity. *Toxicol Appl Pharmacol* (2011) 256(3):300–13. doi: 10.1016/j.taap.2011.06.006
66. Daub S, Lutgens E, Münz T, Daiber A. CD40/CD40L and Related Signaling Pathways in Cardiovascular Health and Disease-The Pros and Cons for Cardioprotection. *Int J Mol Sci* (2020) 21(22):1–18. doi: 10.3390/ijms21228533
67. Chakravorty SJ, Howie AJ, Girdlestone J, Gentle D, Savage CO. Potential Role for Monocyte Chemotactic Protein-4 (MCP-4) in Monocyte/Macrophage Recruitment in Acute Renal Inflammation. *J Pathol* (2001) 194(2):239–46. doi: 10.1002/path.877
68. Beckermann KE, Hongo R, Ye X, Young K, Carbonell K, Healey DCC, et al. CD28 Costimulation Drives Tumor-Infiltrating T Cell Glycolysis to Promote Inflammation. *JCI Insight* (2020) 5(16):1–15. doi: 10.1172/jci.insight.138729
69. Repurposed Antiviral Drugs for Covid-19 — Interim Who Solidarity Trial Results. *New Engl J Med* (2020). doi: 10.1056/NEJMoa2023184
70. Beigel JH, Tomashek KM, Dodd LE, Mehta AK, Zingman BS, Kalil AC, et al. Remdesivir for the Treatment of Covid-19 — Final Report. *New Engl J Med* (2020) 383(19):1813–26. doi: 10.1056/NEJMMc2022236
71. Calfee CS, Matthay MA, Kangelaris KN, Siew ED, Janz DR, Bernard GR, et al. Cigarette Smoke Exposure and the Acute Respiratory Distress Syndrome. *Crit Care Med* (2015) 43(9):1790–7. doi: 10.1097/CCM.0000000000001089

**Conflict of Interest:** The authors declare that the research was conducted in the absence of any commercial or financial relationships that could be construed as a potential conflict of interest.

Copyright © 2021 Laudanski, Jihane, Antalosky, Ghani, Phan, Hernandez, Okeke, Wu, Rader and Susztak. This is an open-access article distributed under the terms of the Creative Commons Attribution License (CC BY). The use, distribution or reproduction in other forums is permitted, provided the original author(s) and the copyright owner(s) are credited and that the original publication in this journal is cited, in accordance with accepted academic practice. No use, distribution or reproduction is permitted which does not comply with these terms.